

# One-step assembly of Re(I) tricarbonyl 2-pyridyltetrazolato metallacalix[3]arene with aqua emission and reversible three-electron oxidation

5 Phillip J. Wright,<sup>a</sup> Sara Muzzioli,<sup>b</sup> Brian W. Skelton,<sup>c</sup> Paolo Raiteri,<sup>a</sup> Jackson Lee,<sup>d</sup> George Koutsantonis,<sup>d</sup> Debbie S. Silvester,<sup>a</sup> Stefano Stagni<sup>b,\*</sup> and Massimiliano Massi<sup>a,\*</sup>

Received (in XXX, XXX) Xth XXXXXXXXXX 20XX, Accepted Xth XXXXXXXXXX 20XX

DOI: 10.1039/b000000x

10 The reaction of 2-pyridyltetrazolate with [Re(CO)<sub>5</sub>X] (X = Cl, Br) yielded the formation of an unexpected cyclic metallacalix[3]arene, as revealed by X-ray structural studies, characterised by aqua emission and reversible three-electron oxidation.

Rhenium(I) tricarbonyl diimine complexes are the focus of intense research for their diverse and readily tunable photophysical and electronic properties.<sup>1</sup> These complexes have found potential applications in a variety of areas including light emitting devices,<sup>2</sup> sensing,<sup>3,4</sup> catalysis,<sup>5</sup> and cellular labeling.<sup>6</sup> The emissive properties of these species have been ascribed to a spin-forbidden radiative decay from metal-to-ligand charge transfer excited states of triplet multiplicity (<sup>3</sup>MLCT).<sup>1</sup> Generally, mononuclear rhenium(I) complexes are the most prevalent in literature.<sup>1</sup> Dinuclear and multinuclear assemblies have also been investigated,<sup>3,7-13</sup> albeit to a lesser extent: in these species the presence of multiple rhenium centres might provide a mechanism for the tuning of the emission characteristics, energy transfer and/or electron transfer.<sup>14-17</sup>

One particular class of multinuclear coordination complexes is represented by the metallacalix[n]arenes,<sup>18</sup> where the metal centres are 20 linked in a cyclic structure by aromatic ligands, thus resembling the analogous calix[n]arenes. While in the case of metallacalix[3]arenes there have been several examples reported with transition metals,<sup>18</sup> rhenium(I)-containing metallacalix[3]arenes are exceptionally rare. In fact, there is only one example reported by Coogan *et al.* of a metallacalix[3]arene containing rhenium(I) tricarbonyl corners and possessing moderate luminescent properties.<sup>19</sup> This assembly was obtained in a three-step synthesis by sequential exchange of two carbonyl ligands and one chloro ligand with a terpyridine-type species (bispyridylpyridone). The variation of the emissive properties of 25 these species could be used in conjunction with host-guest chemistry with sensing purpose.<sup>3,18,19</sup> However, there is a lack of systematic syntheses for luminescent metallacalix[3]arenes with the aim of tuning their photophysical properties and their structural features.

In our research, we have been investigating the photophysical properties of mononuclear tetrazolato and dinuclear tetrazolato-bridged rhenium tricarbonyl complexes, where the rhenium centres are chelated by bidentate 1,10-phenanthroline (**phen**) ligands.<sup>14,20</sup> In furthering this investigation, we intended to use the tetrazole ligand as a bidentate  $\pi$ -acceptor, thus directly involving it as the  $\pi^*$  acceptor 30 in the MLCT excited state. In regards to nitrogen-rich five membered heterocycles, only triazole-containing ligands have been used as diimine systems in luminescent rhenium(I) complexes.<sup>21</sup> Serendipitously, instead of obtaining mononuclear complexes, we isolated the metallacalix[3]arene assembly **1** (Figure 1). The synthesis of this metallacalix[3]arene proceeds readily in a single step and in moderate yields.

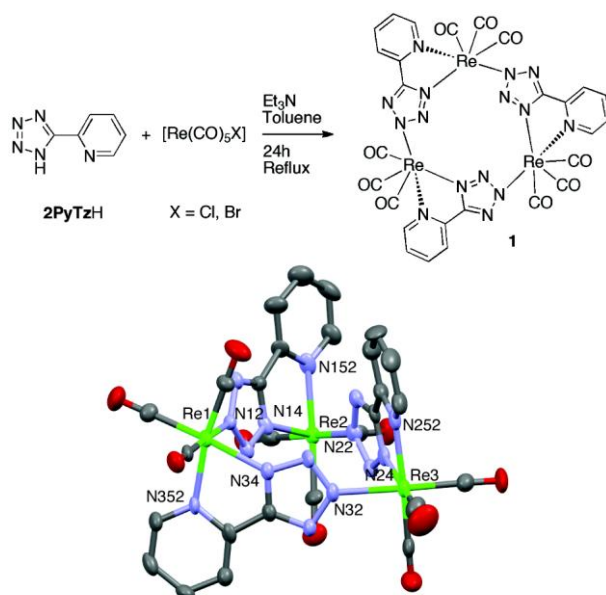


**Figure 1.** One-step synthetic pathway for the formation of the metallacalix[3]arene **1** (top) and crystal structure of **1** with ellipsoids drawn at the 20% probability level. Hydrogen atoms and lattice solvents have been omitted for clarity.

The trinuclear complex **1** was prepared by refluxing  $[\text{Re}(\text{CO})_5\text{X}]$  ( $\text{X} = \text{Cl}, \text{Br}$ ) with 2-(1H-tetrazol-5-yl)pyridine<sup>22</sup> (**2PyTzH**) and triethylamine in toluene under ambient conditions. The formulation and structure of **1** were elucidated by single crystal X-ray diffraction studies<sup>†</sup> (Figure 1), and also supported by NMR and IR spectroscopy as well as elemental analysis. In the solid state, **1** displays a partial cone configuration (*syn, syn, anti*),<sup>18</sup> with one of the **2PyTz** ligand oriented on the opposite side with respect to the other two. The NMR data suggest that the same structure is retained in solution: this is especially evident in considering the three doublets at 9.28, 9.23, and 9.13 ppm corresponding to the H2 atoms of the three pyridine rings.<sup>†</sup> The <sup>13</sup>C NMR spectrum also displays three different patterns of signals relative to the three magnetically non-equivalent **2PyTz** moieties.<sup>†</sup> The IR spectrum shows three intense peaks at 2027, 1916, and 1987  $\text{cm}^{-1}$ , corresponding to the stretching modes of the *facial* CO ligands.

**Table 1.** Photophysical data for **1** from a  $10^{-5}$  M dichloromethane solution

<b>Absorption:</b>	$\lambda_{\text{ab}}$ [nm] ( $10^4 \epsilon$ [ $\text{M}^{-1} \text{cm}^{-1}$ ])	252 (6.3), 283 (4.6), 310 (2.4)
<b>Emission (298 K):</b>	$\lambda_{\text{em}}$ [nm]	498
	$\tau$ [ns] (air)	135
	$\tau$ [ns] (dear)	244
	$\Phi$ (air)	0.030
	$\Phi$ (dear)	0.060
<b>Emission (77 K):</b>	$\lambda_{\text{em}}$ [nm]	466
	$\tau$ [ $\mu\text{s}$ ]	4.99

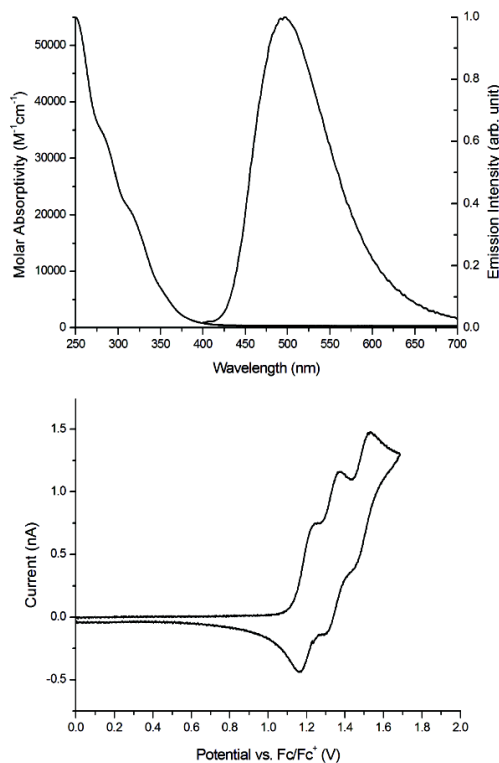
The photophysical data of a *ca.*  $10^{-5}$  M solution of **1** in dichloromethane are summarised in Table 1. The absorption profile (Figure 2) highlights an intense band centred at 250 nm and tailing off into two shoulders in the 280–340 nm region. The lower energy region of this broad band is assigned to an admixture of spin-allowed  $\text{S}_0 \rightarrow {}^1\text{MLCT}$  transitions involving the three rhenium centres and the  $\pi^*$  system of the pyridine rings. The higher energy region might involve ligand centred (LC)  $\pi\text{-}\pi^*$  transitions on the **2PyTz** ligand.

To validate the assignment, the energetics and absorption spectra of the complexes were simulated with time-dependent density functional theory using GAUSSIAN09.<sup>23†</sup> The lowest-energy excited states seem to originate from closely spaced  $\text{HOMO-n} \rightarrow \text{LUMO+m}$  transitions, with  $n = 0-4$  and  $m = 0-2$ . The HOMO- $n$  orbitals are predominantly involving the  $5d(\text{Re})$  orbitals. On the other hand, the LUMO orbitals are localised almost exclusively on the pyridine  $\pi^*$  system.

The emission profile of **1** (Figure 2) evidences a broad and structureless band centred at 498 nm. The relatively long excited state lifetime  $\tau$  suggests that the emission originates from spin-forbidden phosphorescence, and it is therefore assigned to a radiative decay from a triplet  ${}^3\text{MLCT}$  excited state. This conclusion is also supported by the partial quenching of the excited state in the presence of  $\text{O}_2$ . The emission profile is independent from the excitation wavelength and the excited state decay fits satisfactorily with a monoexponential function. These data suggest that the emission originates from a unique excited state, which could be ascribed to the electronically equivalent nature of the three rhenium centres. In a frozen matrix at 77 K, the emission maximum is affected by rigidochromism and it appears blue-shifted by 32 nm, a trend that is consistent with the CT nature of the lowest excited state.<sup>†</sup> Furthermore, the emission profile at 77 K appears rather structureless, suggesting lack of mixing with higher energy LC excited states.

Although the trinuclear species **1** is neutral, it exhibits a rather blue-shifted emission.<sup>1</sup> This can be attributed to the reduction of conjugation within the  $\pi$ -accepting diimine ligand when compared to commonly studied complexes coordinated to **phen** or 2,2'-bipyridine.<sup>24</sup> The consequence is that in **1**, the LUMO orbital is raised in energy with consequent widening of the HOMO-LUMO gap.

Moreover, compared to analogous mononuclear rhenium tetrazolato complexes,<sup>14, 20</sup> the reduction of the  $\sigma$ -donating properties of the doubly coordinated tetrazolato ligand has a stabilising effect on the HOMO orbitals; this conclusion is supported by the relatively higher frequencies of the carbonyl bands.



5 **Figure 2.** Top: absorption and emission profiles of a  $10^{-5}$  M solution of **1** in dichloromethane. Bottom: cyclic voltammogram of **1** in the ionic liquid [1-hexyl-3-methylimidazolium tris(pentafluoroethyl) trifluorophosphate].

Compared to the only other previously reported luminescent metallacalix[3]arene,<sup>19</sup> **1** has a different photophysical behaviour. The emission of **1** is blue-shifted by 59 nm, a trend that can be again explained by the reduction in  $\pi$  conjugation between **2PyTz** and 2,6-bispyridylpyridone. Furthermore, **1** appears as being markedly phosphorescent, since it possesses a longer excited state lifetime (244 vs 20 ns) and higher quantum yield (6% vs 0.2%). These differences can be rationalised by firstly considering the energy gap law: the blue-shifted emission of **1** contributes to a decrease of the non-radiative decay constant ( $k_{nr}$ ). Secondly, the structure of **1** appears more rigid and the reduced degrees of freedom would favour a lower extent of vibronic coupling between the  $^3$ MLCT and the ground state  $S_0$ . These conclusions are supported by direct comparison of the radiative decay ( $k_r = 8.6 \times 10^4$  vs  $2.2 \times 10^5$  s $^{-1}$ ) and non-radiative decay constants ( $k_{nr} = 4.5 \times 10^7$  vs  $7.2 \times 10^6$  s $^{-1}$ ) for **1** and the metallacalix[3]arene previously reported, respectively. On the other hand, when **1** is compared to analogous neutral rhenium tetrazolato complexes, the quantum yield value is not significantly increased despite the blue-shifted emission, which is contravening the energy gap law. This could be rationalised by considering that while widening the HOMO-LUMO gap in **1** indeed decreases the  $k_{nr}$ , it also reduces the gap between the emissive  $^3$ MLCT and deactivating  $^3$ MC states, thus rendering the latter more thermally accessible.

Further investigation into the electrochemical behaviour was performed using cyclic voltammetry for a solution of **1** in the ionic liquid [1-hexyl-3-methylimidazolium tris(pentafluoroethyl) trifluorophosphate].<sup>25</sup> No clearly distinguishable reduction processes could be observed within the scan window of the solvent. On the other hand, three resolved oxidation processes are clearly visible at +1.25 V, +1.36 V, and +1.52 V vs ferrocene/ferrocenium (Fc/Fc $^+$ ) (Figure 2). These processes are ascribed to one-electron oxidation reactions at each individual rhenium centre, e.g. Re(I)  $\rightarrow$  Re(II) + e $^-$ . All three processes show a great deal of reversibility. The peak-to-peak separations for the three redox couples are 87-98 mV (compared to 88 mV for Fc/Fc $^+$ ), suggesting relatively fast kinetics for the electrochemical steps. Formal (midpoint) potentials for the three redox couples were found to be +1.21, +1.32 and +1.47 V vs Fc/Fc $^+$ . If we compare the redox couples of **1** with that of the closest mononuclear analogue available, *fac*-[Re(CO) $_3$ (**phen**)(4-pyridyltetrazolato)]<sup>14</sup> (+1.27 V vs Fc $^+$ /Fc) we see that the subsequent oxidations are apparently affected by the initial removal of an electron. This suggests a significant degree of metal-metal interaction.<sup>26</sup>

In conclusion, the first one-step synthesis of a trinuclear rhenium metallacalix[3]arene promoted by the anionic 2-pyridyltetrazolate is presented. The present metallacalix[3]arene is characterised by radiative decay of aqua colour, originating from  $^3$ MLCT excited states, with long decay lifetime and good quantum yield. These values have been rationalised in terms of reduced conjugation of the  $\pi$  accepting pyridyltetrazolato ligands and structural rigidity. Cyclic voltammetry and TDDFT calculations have been also used to confirm the

interpretation of the photophysical data.

## Notes and references

<sup>a</sup> Department of Chemistry – Curtin University, Kent Street, Bentley 6102 WA, Australia; E-mail: m.massi@curtin.edu.au

<sup>b</sup> Department of Industrial Chemistry "Toso Montanari" – University of Bologna, viale del Risorgimento 4, Bologna 40126, Italy; E-mail:

Stefano.stagni@unibo.it

<sup>c</sup> Centre for Microscopy, Characterisation and Analysis, University of Western Australia, Crawley 6009 WA, Australia;

<sup>d</sup> School of Chemistry and Biochemistry, University of Western Australia, Crawley 6009 WA, Australia.

The work was supported by the Australian Research Council (DP0985481) and Curtin University. PJW is a holder of Australian Postgraduate Award. JL is a holder of Australian Postgraduate Award and partially supported by the Danish National Research Foundation (DNRF93), Center for Materials Crystallography. The authors acknowledge the facilities, scientific and technical assistance of the Australian Microscopy & Microanalysis Research Facility at the Centre for Microscopy, Characterisation & Analysis, The University of Western Australia, a facility funded by the University, State and Commonwealth Governments.

† Electronic Supplementary Information (ESI) available: detailed experimental procedures, X-ray diffraction data, photophysical data, computational calculations. See DOI: 10.1039/b000000x/

<sup>‡</sup> **Crystal data for 1:** Empirical formula C<sub>29</sub>H<sub>16</sub>Cl<sub>4</sub>N<sub>15</sub>O<sub>9</sub>Re<sub>3</sub>. *MW* = 1418.97, Monoclinic, space group *P*2<sub>1</sub>/*n*, *a* = 10.2409(2), *b* = 24.9665(5), *c* = 17.3333(3) Å, β = 91.082(2)°, *V* = 4430.98(15) Å<sup>3</sup>, *Z* = 4, ρ<sub>c</sub> 2.127 g cm<sup>-3</sup>, μ = 8.480 mm<sup>-1</sup>. Reflections collected = 83582, unique reflections = 10698 [*R*(int) = 0.0733]. Max. and min. transmission = 0.784 and 0.61. No. parameters = 569. GoF = 1.320. Final *R* indices [*I* > 2σ(*I*)] *R*1 = 0.0801, *wR*2 = 0.01642, *R* indices (all data) *R*1 = 0.0839, *wR*2 = 0.1659. Largest diff. peak and hole = 4.094 and -1.964 e Å<sup>-3</sup>. CCDC 923692.

1. R. A. Kirgan, B. P. Sullivan and D. P. Rillema, *Top. Curr. Chem.*, 2007, **281**, 45-100.
2. M. Mauro, C. H. Yang, C. Y. Shin, M. Panigati, C. H. Chang, G. D'Alfonso and L. De Cola, *Adv. Mater.*, 2012, **24**, 2054-2058.
3. P. Thanasekaran, C. C. Lee and K. L. Lu, *Acc. Chem. Res.*, 2012, **45**, 1403-1418.
4. S. S. Sun and A. J. Lees, *Coord. Chem. Rev.*, 2002, **230**, 171-192.
5. J. Agarwal, R. P. Johnson and G. H. Li, *J. Phys. Chem. A*, 2011, **115**, 2877-2881.
6. V. Fernandez-Moreira, F. L. Thorp-Greenwood and M. P. Coogan, *Chem. Commun.*, 2010, **46**, 186-202.
7. R. V. Slone, K. D. Benkstein, S. Bélanger, J. T. Hupp, I. A. Guzei and A. L. Rheingold, *Coord. Chem. Rev.*, 1998, **171**, 221-243.
8. K. D. Benkstein, J. T. Hupp and C. L. Stern, *Inorg. Chem.*, 1998, **37**, 5404-5405.
9. S. M. Woessner, J. B. Helms, Y. Shen and B. P. Sullivan, *Inorg. Chem.*, 1998, **37**, 5406-5407.
10. K. D. Benkstein, J. T. Hupp and C. L. Stern, *J. Am. Chem. Soc.*, 1998, **120**, 12982-12983.
11. A. DelNegro, S. Woessner, B. Sullivan, D. Dattelbaum and J. Schoonover, *Inorg. Chem.*, 2001, **40**, 5056-5057.
12. P. Barbazán, R. Carballo, J. S. Casas, E. García-Martínez, G. Pereiras-Gabián, A. Sánchez and E. M. Vázquez-López, *Inorg. Chem.*, 2006, **45**, 7323-7330.
13. Z.-Z. Lu, C.-C. Lee, M. Velayudham, L.-W. Lee, J.-Y. Wu, T.-S. Kuo and K.-L. Lu, *Chem. Eur. J.*, 2012, **18**, 15714-15721.
14. P. J. Wright, S. Muzzioli, M. V. Werrett, P. Raiteri, B. W. Skelton, D. S. Silvester, S. Stagni and M. Massi, *Organometallics*, 2012, **31**, 7566-7578.
15. G. Tapolsky, R. Duesing and T. J. Meyer, *Inorg. Chem.*, 1990, **29**, 2285-2297.
16. R. V. Slone, D. I. Yoon, R. M. Calhoun and J. T. Hupp, *J. Am. Chem. Soc.*, 1995, **117**, 11813-11814.
17. O. Ishitani, K. Kanai, Y. Yamada and K. Sakamoto, *Chem. Commun.*, 2001, 1514-1515.
18. E. Zangrando, M. Casanova and E. Alessio, *Chem. Rev.*, 2008, **108**, 4979-5013.
19. M. Coogan, V. Fernández Moreira, B. M. Kariuki, S. J. A. Pope and F. L. Thorp-Greenwood, *Angew. Chem. Int. Ed.*, 2009, **48**, 4965-4968.
20. M. V. Werrett, D. Chartrand, J. D. Gale, G. S. Hanan, J. G. MacLellan, M. Massi, S. Muzzioli, P. Raiteri, B. W. Skelton, M. Silberstein and S. Stagni, *Inorg. Chem.*, 2011, **50**, 1229-1241.
21. C. B. Anderson, A. B. S. Elliott, C. J. McAdam, K. C. Gordon and J. D. Crowley, *Organometallics*, 2013, **32**, 788-797.
22. K. Koguro, T. Oga, S. Mitsui and R. Orita, *Synthesis*, 1998, 910-914.
23. M. J. Frisch et al., *Gaussian 09, Revision C.01*, (2010) Gaussian Inc., Wallingford CT.
24. L. A. Casson, S. Muzzioli, P. Raiteri, B. W. Skelton, S. Stagni, M. Massi and D. H. Brown, *Dalton Trans.*, 2011, **40**, 11960-11967.
25. D. S. Silvester, S. Uprety, P. J. Wright, M. Massi, S. Stagni and S. Muzzioli, *J. Phys. Chem. C*, 2012, **116**, 7327-7333.
26. F. Paul, W. E. Meyer, L. Toupet, H. J. Jiao, J. A. Gladysz and C. Lapinte, *J. Am. Chem. Soc.*, 2000, **122**, 9405-9414.